Deep Learning Techniques for Lung Cancer Recognition

Suseela Triveni Vemula
Department of Mathematics, Geethanjali College of Engineering and Technology, Hyderabad, Telangana, India
vstriveni@gmail.com

Maddukuri Sreevani
Department of CSE, BVRIT Hyderabad College of Engineering for Women, Bachupally, Hyderabad, Telangana, India
sreevani.m@bvrithyderabad.edu.in

Perepi Rajarajeswari
Department of Software Systems, School of Computer Science and Engineering, Vellore Institute of Technology, Vellore, Tamil Nadu, India
rajacse77@gmail.com (corresponding author)

Kumbham Bhargavi
Department of CSE (AI &ML), Faculty of Keshav Memorial Institute of Technology, Hyderabad, Telangana, India
bhargavikumbham@gmail.com

Joao Manuel R. S. Tavares
Instituto de Ciencia e Inovacao em Engenharia Mecanica e Engenharia Industrial, Departamento de Engenharia Mecanica, Faculdade de Engenharia, Universidade do Porto, Portugal
tavares@fe.up.pt

Sampath Alankritha
Department of Computer Science and Engineering, School of Computer Science and Engineering, Vellore Institute of Technology, Vellore, Tamil Nadu, India
sampathalankritha@gmail.com

Received: 16 April 2024 | Revised: 1 May 2024 and 6 May 2024 | Accepted: 7 May 2024

 DOI: https://doi.org/10.48084/etasr.7510

ABSTRACT

Globally, lung cancer is the primary cause of cancer-related mortality. Higher chance of survival depends on the early diagnosis of lung nodules. Manual lung cancer screenings depends on the human factor. The variability in size, texture, and shape of lung nodules may pose a challenge for developing accurate automatic detection systems. This article proposes an ensemble approach to tackle the challenge of lung nodule detection. The goal was to improve prediction accuracy by exploring the performance of multiple transfer learning models instead of relying solely on deep learning models. An extensive dataset of CT scans was gathered to train the built deep learning models. This research paper is focused on the Convolutional Neural Networks' (CNNs') ability to automatically learn and adapt to discernible features in the lung images which is particularly beneficial for accurate classification, aiding in identifying true and false labels, and ultimately enhancing lung cancer diagnostic accuracy. This paper provides a comparative analysis of the performance of CNN, VGG-16, and VGG-19. Notably, the built transfer learning model VGG-16 achieved a remarkable accuracy of 95%, surpassing the baseline method.

Keywords-image processing; image classification; deep learning; transfer learning

I. INTRODUCTION

Lung cancer holds a prominent position in the landscape of global health, being responsible for most cancer-related fatalities and will remain a significant health concern for the foreseeable decades [1]. Timely identification and precise diagnosis are pivotal in enhancing patient outcomes [2, 3]. The five year survival rate for individuals diagnosed with lung cancer stands at a modest 10% to 20%. Medical procedures such as Computed Tomography (CT) and MRI scans are commonly employed for early detection, significantly contributing to patient survival rates [4, 5]. Previously, advanced methods like the Sequential Flood Feature Selection Algorithm (SFFSA) and Genetic Algorithm (GA), which have historically served as the cornerstones of intelligent processes, have been employed for optimal feature extraction [6]. While CT remains the benchmark for lung nodule detection, it has limitations, notably involving a propensity for high false-positive results and the emission of potentially harmful X-ray radiation. In response to these concerns, LDCT has been proposed to mitigate the risks associated with radiation while detecting lung cancer. However, it is worth noting that cancer-related deaths have been more prevalent among individuals undergoing LDCT screening. Another significant development in this field is the emergence of the 2-deoxy-18F-fluorodeoxyglucose (18F-FDG) PET, designed to enhance the accuracy of lung cancer detection [6]. This imaging technique provides semi-quantitative data on tumor glucose metabolism, which proves valuable in diagnosing Non-Small Cell Lung Cancer (NSCLC). Authors in [7] harnessed deep residual learning techniques to create a method for detecting lung cancer in CT images. Their approach involved employing UNet and ResNet models within a preprocessing pipeline to emphasize and extract features from lung areas exhibiting signs of cancer. The LIDC-IRDI method demonstrated an 84% increase in accuracy compared to conventional techniques [5]. Authors are focused on developing an Optimal Deep Neural Network (ODNN) to enhance the accuracy of lung CT scan analysis by reducing the number of characteristics and comparing it with other classification algorithms [8]. Their research revealed a significant improvement in the performance of Machine Learning (ML) algorithms regarding the precise detection of normal and abnormal lung images. Specifically, their findings indicate a peer specificity of 94.56%, an accuracy level of 96.2%, and a sensitivity level of 94.2%. These impressive statistics demonstrate the feasibility of ameliorating cancer detection in CAT scans [9], underscoring the success of their research in this regard.

Authors in [10] emphasized the significant role of image processing techniques in lung cancer diagnosis. They employed Deep Learning (DL) methodologies to advance the study of this prevalent and life-threatening disease. The proposed method utilizes CT, PET, and X-ray images, and demonstrated an accuracy rate of up to 80%. Several authors have thoroughly examined and evaluated methods that identify and categorize cellular breakdown in the lungs [11, 12]. Numerous specialists have gone through extensive learning processes [13] to aid radiologists in reaching more precise conclusions. Previous studies have confirmed that computer-aided design frameworks developed based on DL paradigms can significantly improve the efficiency and accuracy of clinical findings, particularly for various prevalent disease types such as lung and bosom malignant growth [14, 15]. Previous studies focused on the DL-based CADD frameworks can automatically extract important level elements from original images using recognizable organizational models, especially when compared to conventional CADD frameworks. Nevertheless, it is critical to understand that DL-based CADD frameworks have unique limitations, including low awareness, exaggerated but misleading benefits, and substantial time consumption. Authors in [16] proposed the adoption of image processing techniques, like filters and edge-preserving methods, to enhance the quality of lung scans, especially grayscale images, which could lead to clearer analysis and more reliable diagnoses. Inspired by the success of remote lung cancer detection, they recommended exploring cloud computing for ML-based remote diagnosis. Cloud computing power allows efficient processing and analysis of large medical datasets. For improved feature extraction and classification, the researchers suggest employing a Deep Belief Network (DBN) optimized by the Cat Swarm Optimization (SCO) algorithm [17]. The lung cancer detection system in [18] operates in three stages. First, it gathers data using cameras and sensors. Then, these data are fed into ML and DL algorithms like RF, LSTM, and LR. These algorithms act like intelligent tools that sift through the data to find patterns. Finally, the system's performance is evaluated using metrics like R-squared, RMSE, and MAE. These metrics provide a score indicating how accurate the system is at detecting cancer. This method resulted in a significant improved accuracy of 93.52%. The proposed method in [19] displayed promising results, even when compared against two of the top ML models for prediction in this field. Since unbalanced data can affect accuracy, the technique called SMOTEND was put into service to address this issue. Experiments revealed that the new approach achieved a lower error rate (0.195) with MLP compared to CNN, suggesting that MLP performed better in this specific task.

DL techniques are widely used in conjunction with data mining. In this context, creating a structured reporting system can greatly benefit ML and DL objectives. Authors in [20] conducted a review that utilized continuous monitoring to predict cellular lung breakdown. They employed an expansion method based on fluffy groups in addition to order. To achieve precise picture segmentation, fuzzy grouping must be deployed.

This paper highlights the strengths of a Lung Cancer Classification System that classifies the process and yields promising results, showcasing the effectiveness of DL models in identifying cancerous patterns in CT images. Among the models, VGG-16 demonstrated superior performance, emphasizing its ability to capture intricate features crucial for accurate lung cancer classification. This paper highlights the current state of the art DL approaches for the prediction of lung cancer. Still many difficulties are faced, entailing privacy protection issues, clinical verification on a large scale, and legal issues.

The main aspects of this research paper are:

- The challenge of lung nodule detection is addressed by introducing an ensemble approach.
- An extensive dataset of CT scans was gathered to train built DL models. CNNs were trained to differentiate between cancerous and non-cancerous images using this dataset.
- The proposed Deep CNN and transfer learning models were validated through distinct training, validation, and testing datasets.

II. THE PROPOSED METHODOLOGY

The proposed system employs an Ensemble approach to enhance lung nodule detection. DL CNN models, specifically VGG-16, VGG-19, and Mobilenet, are implementd to analyze an extensive dataset of CT scans. The proposed transfer learning model, VGG-16, has demonstrated a remarkable 95% accuracy, surpassing the baseline methods. Figure 1 portrays the recommended architectural framework, which aims to greatly enhance early diagnosis by combining various high-performing algorithms.

A. Data Collection

The dataset was purposefully constructed to enable the investigation of various approaches for the analysis of patterns in CT image data related to contrast use and patient age. The common main goal is to find image textures, statistical patterns, and characteristics that disclose significant relationships with these properties. Creating efficient systems that can automatically categorize incorrectly classified images or recognize outliers that can point to questionable instances, erroneous measurements, or miscalibrated machinery is the ultimate objective. The dataset, which includes the middle slice of CT scans with age, modality, and contrast tags, was created by taking a subset of images from the Cancer Imaging archive [21]. The latter includes 475 series from 69 different patients.

B. Data set Description

- Gender G, specifies the person's sex.
- Age A gives a person's age.
- Smoking S determines whether the person is a smoker or not.
- Yellow fingers Y refers to whether the person has yellow fingers or not.
- Anxiety A shows if the person is anxious or not.
- Alcohol Al represents if the person consumes alcohol or not.
- Coughing C refers to whether the person suffers from coughing or not.
- Shortness of breath SOB refers to whether the person has shortness of breath or not.
- Chest Pain CP shows whether the person has chest pain or not.
- Lung Cancer LC shows if the person has been diagnosed with lung cancer or not.

All the features are nominal except for age, which is numerical. Table I shows a sample of the dataset, while Figure 1 presents the LC positive and negative images. Subsequently, the values were normalized.

TABLE I. DATA SAMPLE

S.no	G	A	S	Y	A	Al	C	SOB	CP	LC
1	M	69	2	2	2	2	2	2	2	Yes
2	F	74	1	1	2	1	1	1	1	No
3	M	60	1	1	1	1	1	1	1	No
4	F	63	2	1	2	1	2	1	2	Yes
5	M	65	1	2	1	1	1	2	1	Yes

TABLE II. DATA AFTER NORMALIZATION

S.no	G	A	S	Y	A	Al	C	SOB	CP	LC
321	1	0.6785	1	1	1	0	0	1	0	Yes
336	1	0.7896	0	0	1	0	1	1	1	No
334	0	0.2093	1	0	0	0	0	1	0	No
151	0	0.2316	1	1	0	0	0	0	0	Yes
314	1	0.8976	1	0	0	1	1	1	1	Yes

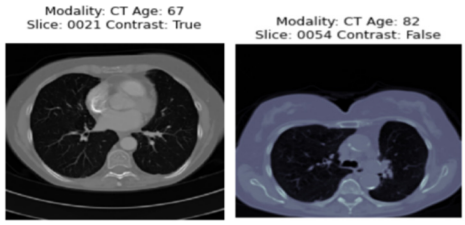

Fig. 1. "Yes" and "No" 'LC images.

C. Data Preprocessing

In the data preprocessing stage for lung cancer image classification with true or false labels, several essential steps are undertaken to ensure the effectiveness of subsequent ML models. Initially, the collected images are carefully preprocessed to a standardized resolution, mitigating inconsistencies across the dataset. Image augmentation techniques, such as rotation, flipping, and scaling are applied to address potential noise and enhance model's robustness. Subsequently, the images are normalized to a common intensity scale, optimizing their compatibility for neural network training. The training set is further diversified by adding random variations to augment the dataset and minimize overfitting. Additionally, the dataset is split into training, validation, and testing subsets, enabling the model to learn, tune, and evaluate its performance on distinct subsets of data. This meticulous preprocessing pipeline lays the foundation for accurate and reliable lung cancer image classification, ensuring the model can discern between true and false labels with heightened precision. CT images are often obtained as separate scans and may be misaligned. Various artifacts, such as motion artifacts in CT scans, may affect these images. Image registration is used to ensure spatial alignment between two photographs. The symmetric normalization (SyN) function is commonly deployed for nonlinear picture registration. We utilized the SyN function to handle deformations and improve image alignment. The SyN function takes the CT anatomical data. It employs forward transformation to generate the images.

A similarity metric compares the source and target images. To generate the normalized image, the SyN function performs cross-correlation computation. The SyN equations are given below.

$$I_t = SyN\ (I_t, \emptyset_1, \emptyset_2),\ i= 1,\ldots.., n \quad (1)$$

The resample image filter function standardizes the CT image dimensions and supports the proposed model to achieve a meaningful outcome. The mathematical equation for the resampling process of the image is:

$$I_t = Resample\_\ Image\_\ Filter\ (\ I_t, s, scale, NI), \quad (2)$$

$$i = 1,\ldots., n$$

After reading the CT picture from each subset, the values which were greater than 1,200 HU and less than 600 HU were filtered out standardizing the results to fall between 0 and 1.

D. Data Splitting

When applying ML algorithms to make predictions on data that were not used to train the model, the train-test split procedure is followed to estimate their performance. This procedure can be performed quickly and easily, allowing the comparison of the performance of ML algorithms for predictive modeling problem. Training and test datasets are described with the help of the patient's characteristics.

E. Model Building

CNN Model: The image classification task for lung cancer diagnosis relies heavily on CNNs. In the considered model, the Max pooling layers come after three convolutional layers. The convolutional layer's output is flattened using a flatten layer. The output of the flattened layer will come next and will have two fully connected layers. To enable reliable and quick training, a few batch normalization layers were added. To prevent overfitting, a dropout layer was included before the final layer. Soft probabilities for each of the two classes are produced by the output layer, which is the last layer.

TABLE III. DETAILS OF THE CNN

	Layer Type	**Output Shape**	**Param**
1	Cov2d(Conv 2D)	(None, 256,32)	2435
2	Max_Pooling 2d(MaxPooling2D)	(None,128,128,32)	0
3	Conv2d_1(Conv2D)	(None,128,128,64)	16596
4	Max_Pooling2d_1 (Max Pooling 2D)	(None,64,64,64)	0
5	9 conv2d_2(Conv2D)	(None,64,64,128)	74956
6	Max_pooling2d_2 (Max Pooling 2D)	(None,32,32,128)	0
7	Flatten(flatten)	(None, 131072)	0
8	Dense(Dense)	(None, 256)	44554677
9	Batch_normalization (BatchN normalization)	(None, 256)	1014
10	Dense_1(Dense)	(None, 256)	35696
11	Dropout(dropout)	(None, 128)	0
12	Batch_normalization_1 (batchnormalization)	(None, 128)	515
13	Dense_2(Dense)	(None, 3)	397

CNNs employ convolutional layers that systematically scan and extract intricate features from the input lung images. The network learns hierarchical representations, discerning nuanced patterns, and textures crucial for distinguishing between cancerous and non-cancerous regions. Using pooling layers, spatial dimensions are reduced, allowing the model to focus on the most salient features. The extracted features are then flattened and fed into the fully connected layers, enabling the network to learn complex relationships and make predictions. The CNN's ability to automatically learn and adapt to discernible features in the lung images is particularly beneficial for accurate classification, aiding in identifying true and false labels and ultimately enhancing lung cancer diagnostic accuracy. Details of the employed 2D CNN architecture are presented in Table III.

F. VGG-16 Model

The vgg-16 model utilizes a deep CNN architecture specifically designed for image classification tasks. Comprising 16 layers, including 13 convolutional layers (5 ReLu layers, 5 max-pooling layers, and 3 fully connected layers), with a softmax output layer, vgg-16 excels at capturing intricate patterns and features within images. In the context of lung cancer image classification, vgg-16 processes the input images through a series of convolutional and pooling layers, gradually extracting hierarchical features. This model is particularly adept at learning complex representations, making it well-suited for discerning subtle patterns indicative of lung cancer. The final fully connected layers then leverage these learned features to classify the images into true or false labels..

G. VGG-19 Model

The VGG-19 model, a deep CNN, operates effectively in lung cancer image classification by leveraging its deep architecture. Comprising 19 layers, VGG-19 excels at capturing intricate features within images, a critical capability for discerning nuances in lung cancer images. The convolutional layers in the model perform successive operations to extract hierarchical features and the fully connected layers aid in the final classification. VGG-19 manifests its strength in lung cancer classification by automatically learning and recognizing intricate patterns, textures, and statistical features from CT scans. The model's deep architecture allows it to accurately differentiate between true and false labels, making it a robust solution for accurate lung cancer image classification. In summary, VGG-19's proficiency in lung cancer image classification lies in its ability to extract and comprehend complex features from medical images, making it able to distinguish between true and false labels precisely. The model's deep architecture empowers it to capture subtle details crucial for accurate classification, rendering it an asset in medical image analysis.

III. RESULT ANALYSIS

A. Data Exploration

Data exploration analysis was performed regarding gender, smoking, anxiety, yellow fingers, chest pain, alcohol, coughing, and shortness of breath. Figures 2-3 exhibit some of the studied patients' data.

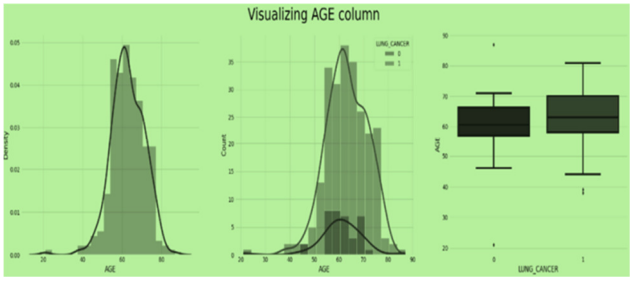

Fig. 2. Visualization of the studied patients' age.

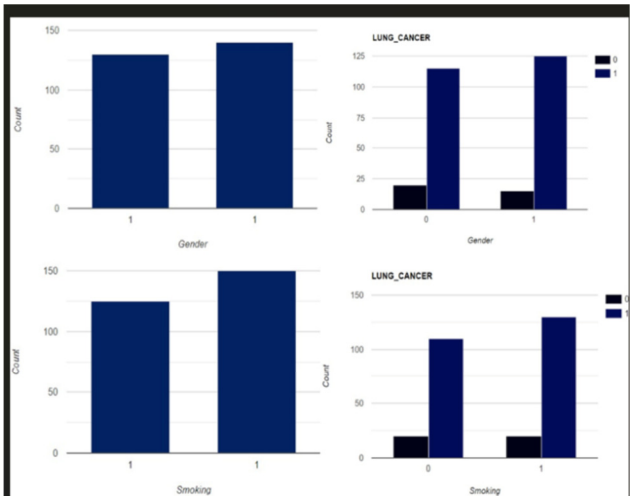

Fig. 3. Visualization of the studied patients' gender and smoking habits.

B. Comparative Analysis of the Performance of CNN, VGG-16, and VGG-19

For the considered lung cancer image classification process, the performance of three distinct deep learning models, CNNs, VGG-16, and VGG-19, was evaluated. The baseline CNN exhibited a respectable accuracy of 87%, demonstrating its ability to identify lung cancer features within the dataset. Further analysis revealed shortcomings in discerning subtle patterns, resulting in some misclassifications. VGG-16 and VGG-19 performed significantly better than the baseline. VGG-16 achieved an impressive accuracy of 95%, leveraging its deeper architecture to capture intricate features, thereby enhancing its ability to classify lung images accurately. VGG-19, while slightly less accurate at 92%, demonstrated a balance between model complexity and performance. The nuanced differences between these models call for a closer examination of additional performance metrics. To understand the models' overall performance across True Positives (TP), True Negatives (TN), False Positives (FP), and False Negatives (FN), it is necessary to evaluate specificity, precision, recall, and F1 score. These metrics give a more detailed analysis of each model's strengths and weaknesses, which guides further optimization for accurate lung cancer classification. VGG-16, with its superior accuracy, showed heightened sensitivity, minimizing false negatives crucial for lung cancer detection.

Accuracy is the ratio of corrected predicted instances to the total number of instances in the datasets:

$$\text{Accuracy}=\frac{TP+TN}{TP+TN+FP+FN} \quad (3)$$

Recall is the ratio of correctly predicted positive instances to all actual positive instances:

$$\text{Recall}=\frac{TP}{TP+FN} \quad (4)$$

Precision is the ratio of correctly predicted positive instances to all positive instances:

$$\text{Precision}=\frac{TP}{TP+FP} \quad (5)$$

F1 score is the harmonic mean of precision and recall:

$$\text{F1 score}=2\frac{\text{Precision}\times\text{Recall}}{\text{Precision}+\text{Recall}} \quad (6)$$

Table IV presents the performance comparison across the studied DL models. The precision, recall scores, and F1 score values for the different models are portrayed in Figures 4 and 5.

The classification report can be performed in the form of a matrix by utilizing the confusion matrix. By deploying the concept of binary classification, four combinations of data categories can be formed. These are denoted as TP, TN, FP, and FN. The confusion matrices for CNN, VGG-16, VGG-19 model are depicted in Figures 6-8. VGG-16 was proved to be the superior model. Figure 9 discloses the accuracy and loss of the considered models.

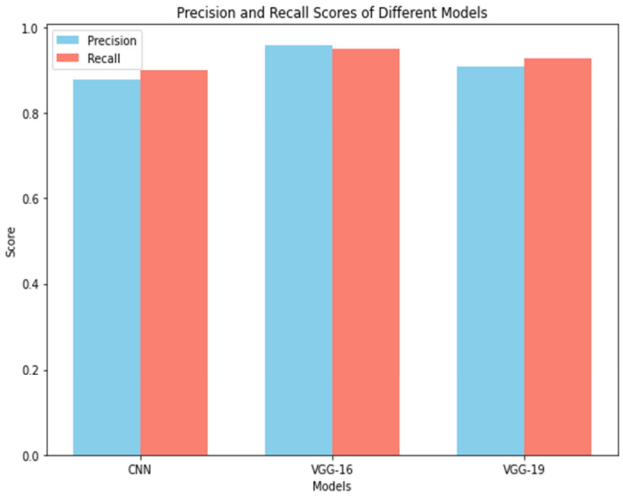

Fig. 4. Precision and recall scores of the studied DL models.

TABLE IV. PERFORMANCE COMPARISON OF THE STUDIED DEEP LEARNING MODELS

Model	Accuracy	Precision	Recall	F1-score
CNN	0.87	0.88	0.90	0.89
VGG-16	0.95	0.96	0.95	0.95
VGG-19	0.92	0.91	0.93	0.92

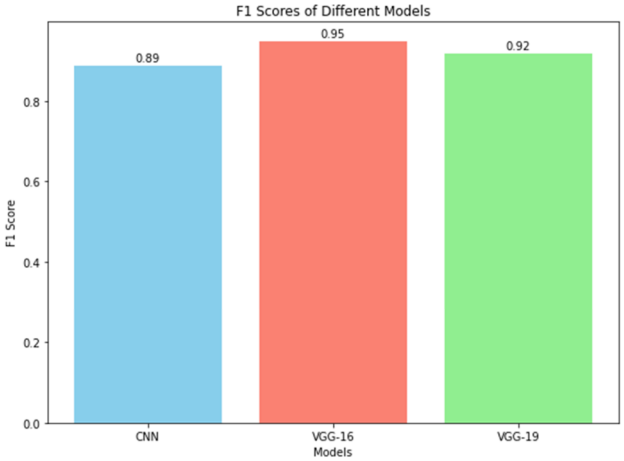

Fig. 5. F1 scores of the studied deep learning models.

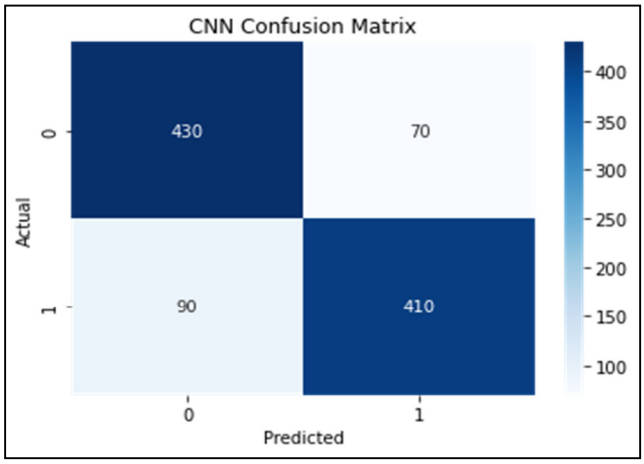

Fig. 6. CNN model's confusion matrix.

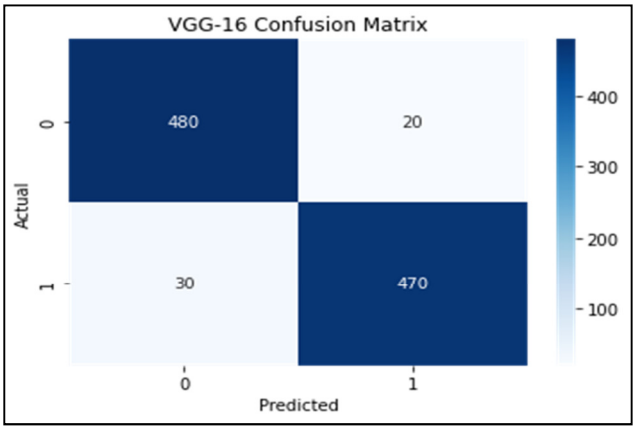

Fig. 7. VGG-16 model's confusion matrix.

C. Statistical Analysis

In the detection performance test, metrics were evaluated on a per-lesion basis. The FROC curve (Figure 10) was employed to evaluate whether the bounding boxes proposed by the model accurately identified malignant cancers in radiographs. The vertical axis of the FROC curve is sensitivity and the horizontal axis is mFPI, which is the number of FPs divided by the number of radiographs in the dataset.

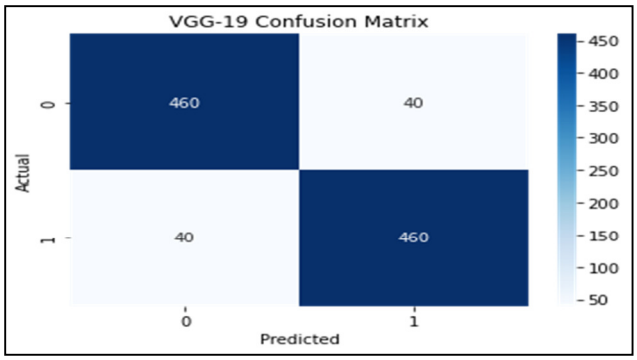

Fig. 8. VGG-19 model's confusion matrix.

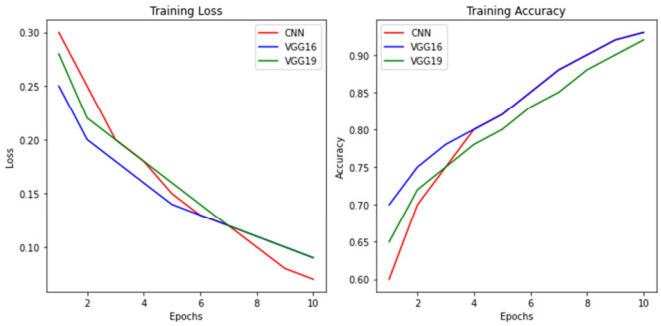

Fig. 9. Obtained accuracy and loss of CNN, VGG 16, and VGG19.

Fig. 10. FROC curve for the test dataset.

IV. CONCLUSION AND FUTURE WORK

In conclusion, the proposed lung cancer image classification process has yielded promising results, showcasing the effectiveness of Deep Learning (DL) models in identifying cancerous patterns in Computed Tomography (CT) images. The baseline Convolutional Neural Network (CNN) model had a commendable accuracy of 87%, but the more sophisticated architectures, VGG-16, and VGG-19, exhibited significant improvements with accuracy scores of 95% and 92%, respectively. VGG-16 demonstrated superior performance, emphasizing its ability to capture intricate features, crucial for accurate lung cancer classification. The comprehensive analysis of performance metrics, including

sensitivity, precision, recall, and F1 score, provided a nuanced understanding of each model's strengths and weaknesses.

Moving forward, several avenues for future work can enhance the robustness and applicability of a lung cancer classification system. Initially, exploring additional deep learning architectures and transfer learning models could be undertaken to optimize performance further. Integration of ensemble techniques, combining predictions from multiple models, may enhance overall accuracy and reliability.

ACKNOWLEDGMENT

We are sincerely thankful to the Academic Institution for supporting this research work.

[1] C. P. Davis, "Cancer: Symptoms, Causes, Treatment, Stages, Prevention," Oct. 10, 2023. https://www.medicinenet.com/cancer/article.htm.

[2] *Latest global cancer data: Cancer burden rises to 18.1 million new cases and 9.6 million cancer deaths in 2018*. Geneva, Switzerland: International agency for research on cancer, 2018.

[3] Dr. B. Mesko, "Top AI Algorithms In Healthcare," *The Medical Futurist*, Apr. 25, 2023. https://medicalfuturist.com/top-ai-algorithms-healthcare/ .

[4] S. K. Lakshmanaprabu, S. N. Mohanty, K. Shankar, N. Arunkumar, and G. Ramirez, "Optimal deep learning model for classification of lung cancer on CT images," *Future Generation Computer Systems*, vol. 92, pp. 374–382, Mar. 2019, https://doi.org/10.1016/j.future.2018.10.009.

[5] J. Alam, S. Alam, and A. Hossan, "Multi-Stage Lung Cancer Detection and Prediction Using Multi-class SVM Classifie," in *2018 International Conference on Computer, Communication, Chemical, Material and Electronic Engineering (IC4ME2)*, Feb. 2018, pp. 1–4, https://doi.org/10.1109/IC4ME2.2018.8465593.

[6] M.Gomathi and P. Thangaraj, "A computer aided diagnosis system for detection of lung cancer nodules using extreme learning machine," *International Journal of Engineering Science and Technology*, vol. 2, no. 10, pp. 5770-5779, Oct. 2010.

[7] F. Mlawa, E. Mkoba, and N. Mduma, "A Machine Learning Model for detecting Covid-19 Misinformation in Swahili Language," *Engineering, Technology & Applied Science Research*, vol. 13, no. 3, pp. 10856–10860, Jun. 2023, https://doi.org/10.48084/etasr.5636.

[8] R. Alkadi, F. Taher, A. El-baz, and N. Werghi, "A Deep Learning-Based Approach for the Detection and Localization of Prostate Cancer in T2 Magnetic Resonance Images," *Journal of Digital Imaging*, vol. 32, no. 5, pp. 793–807, Oct. 2019, https://doi.org/10.1007/s10278-018-0160-1.

[9] C. Haarburger, P. Weitz, O. Rippel, and D. Merhof, "Image-Based Survival Prediction for Lung Cancer Patients Using CNNS," in *2019 IEEE 16th International Symposium on Biomedical Imaging (ISBI 2019)*, Apr. 2019, pp. 1197–1201, https://doi.org/10.1109/ISBI.2019.8759499.

[10] D. Paredes, A. Saha, and M. A. Mazurowski, "Deep learning for segmentation of brain tumors: can we train with images from different institutions?," in *Medical Imaging 2017: Computer-Aided Diagnosis*, Mar. 2017, vol. 10134, pp. 430–435, https://doi.org/10.1117/12.2255696.

[11] K. Awai *et al.*, "Pulmonary nodules at chest CT: effect of computer-aided diagnosis on radiologists' detection performance," *Radiology*, vol. 230, no. 2, pp. 347–352, Feb. 2004, https://doi.org/10.1148/radiol.2302030049.

[12] S. Cheran and G. Gargano, "Computer aided diagnosis for lung CT using artificial life models," Oct. 2005, Art. no. 4, https://doi.org/10.1109/SYNASC.2005.28.

[13] W. Ausawalaithong, S. Marukatat, A. Thirach, and T. Wilaiprasitporn, "Automatic Lung Cancer Prediction from Chest X-ray Images Using Deep Learning Approach," in *2018 11th Biomedical Engineering International Conference (BMEiCON)*, Nov. 2018, pp. 1–5, https://doi.org/10.1109/BMEiCON.2018.8609997.

[14] X. Zhao, Y. Wu, G. Song, Z. Li, Y. Zhang, and Y. Fan, "A deep learning model integrating FCNNs and CRFs for brain tumor segmentation," *Medical Image Analysis*, vol. 43, pp. 98–111, Jan. 2018, https://doi.org/10.1016/j.media.2017.10.002.

[15] M. Havaei *et al.*, "Brain tumor segmentation with Deep Neural Networks," *Medical Image Analysis*, vol. 35, pp. 18–31, Jan. 2017, https://doi.org/10.1016/j.media.2016.05.004.

[16] M. S. Kumar and K. V. Rao, "Prediction of Lung Cancer Using Machine Learning Technique: A Survey," in *2021 International Conference on Computer Communication and Informatics (ICCCI)*, Jan. 2021, pp. 1–5, https://doi.org/10.1109/ICCCI50826.2021.9402320.

[17] M. A. Thanoon, M. A. Zulkifley, M. A. A. Mohd Zainuri, and S. R. Abdani, "A Review of Deep Learning Techniques for Lung Cancer Screening and Diagnosis Based on CT Images," *Diagnostics*, vol. 13, no. 16, Jan. 2023, Art. no. 2617, https://doi.org/10.3390/diagnostics13162617.

[18] A. S. Alkarim, A. S. A.-M. Al-Ghamdi, and M. Ragab, "Ensemble Learning-based Algorithms for Traffic Flow Prediction in Smart Traffic Systems," *Engineering, Technology & Applied Science Research*, vol. 14, no. 2, pp. 13090–13094, Apr. 2024, https://doi.org/10.48084/etasr.6767.

[19] W. Alkaberi and F. Assiri, "Predicting the Number of Software Faults using Deep Learning," *Engineering, Technology & Applied Science Research*, vol. 14, no. 2, pp. 13222–13231, Apr. 2024, https://doi.org/10.48084/etasr.6798.

[20] B. H. Bhavani and N. C. Naveen, "An Approach to Determine and Categorize Mental Health Condition using Machine Learning and Deep Learning Models," *Engineering, Technology & Applied Science Research*, vol. 14, no. 2, pp. 13780–13786, Apr. 2024, https://doi.org/10.48084/etasr.7162.

[21] K. S. Mader, "CT Medical Images," *kaggle*, 2017. https://www.kaggle.com/datasets/kmader/siim-medical-images.